

A. Shimada¹, I. Otsuka¹, N. Fujii² and T. Saito²

¹*Sustainable Environmental Studies, Graduate School of Life and Environment Sciences, University of Tsukuba*

²*Research Reactor Institute, Kyoto University*

INTRODUCTION: A historical riddle about chiral homogeneity, the origin of L-dominant amino acids in biological world, has intrigued scientists for many years, though there has been no general consensus as yet to it. Life could not be born without homochirality, that is to say, no homochirality – no life. However, we cannot imagine at all when and how the homochirality was established on early earth. Amino acids are stereochemically too labile to retain their homochiral state in natural environment because racemization pressure is overwhelmingly strong, especially in aqueous solution. An elaborate mechanism is necessary to put biological world into homochirally-stable state. The homochirality of contemporary biological world is fully guaranteed by enzyme enantioselectivity. Since the enzyme enantioselectivity has remained unclear, a deeper understanding of its mechanism is required to unravel all the riddle of the origin of homochirality. We have so far researched a mechanism of tryptophanase (TPase) enantioselectivity, with the aim of answering this difficult problem. TPase degrades L-tryptophan (L-Trp) by β -elimination reaction, and also synthesizes L-Trp from L-serine (L-Ser) and indole by β -replacement reaction by use of its absolute enantioselectivity. On the other hand, it is perfectly inert to D-tryptophan (D-Trp) and D-serine (D-Ser) at all. Additionally these D-amino acids inhibit TPase in L-Trp degradation and L-Trp synthesis from L-Ser. The present report describes to focus simply on D-Ser acting on TPase as a competitive inhibitor.

EXPERIMENTAL: Generally speaking, D-amino acid works as inactive or inhibitor against enzyme. D-Ser completely has no reaction to TPase. When TPase synthesizes L-Trp from L-Ser and indole, D-Ser inhibits the synthetic reaction. Since kinetic analysis was effective to probe the interaction between D-Ser and TPase, we analyzed D-Ser behavior against TPase in L-Trp synthesis in terms of it. For kinetics, reaction was conducted at 50 °C for 4 hr in Dry Thermo Unit DTU-1B with 0, 0.1, 0.2, 0.3, 0.6, or 1 M of D-Ser added in reaction mixtures that were prepared by combining the required L-Ser (10-100 mM) with fixed apotryptophanase (apoTPase, 0.46 μ M), indole (5.4 mM) and pyridoxal 5'-phosphate (PLP) concentrations (0.4 mM) in 500 μ L of 0.1 M potassium phosphate buffer (PB), adjusted to a pH of 8.3. After 4hr, the reaction mixture was cool on

ice to stop reaction. 200 μ L of the reaction mixture was filtered through Amicon Ultra Centrifugal Filters cutting more than MW 3000, immediately injected on a Crownpack CR (+) Resolution HPLC resolution column equilibrated with the degassed eluent through a Degaser, and eluted at a flow rate of 0.9 mL/min at room temperature with an HPLC pump. L-Trp synthesis from L-Ser was determined measuring with a CD-1595 detector. Ellipticity $[\theta]$ was monitored at $\lambda = 230$ nm with the CD detector, represented in units of mdeg. Ellipticity of the eluent was set up to zero at a wavelength of $\lambda = 230$ nm, so the peaks of L-Trp appeared on the positive side.

RESULTS AND DISCUSSION: For kinetic analysis, TPase activity on L-Trp synthesis was assayed in triplicate at the same substrate concentration, averaged. Lineweaver-Burk plots were drawn based on the least squares method. The reciprocal of rate constant (ordinate) versus the reciprocal of substrate concentration (abscissa) was plotted for each concentration of D-Ser, depicting a typical competitive inhibition plot. Kinetic constants were calculated from these double-reciprocal plots, and also an inhibition constant K_I of D-Ser was determined from their slopes. K_m was 44 mM, V_m 2.2×10^{-4} mM/s, k_{cat} 0.48/s and K_I 419 mM. D-Ser is a competitive inhibitor against TPase in L-Trp synthesis reaction from L-Ser and indole. Competitive inhibitor usually shares a highly structural resemblance with its substrate. D-Ser stereostructure fits into the active site structure of TPase, promptly binding there. Although D-Ser can bind with the active site, D-Ser is not involved in L-Trp synthetic reaction. Perhaps D-Ser cannot form aldimine-bond with PLP at the first step of L-Trp synthesis. However, our previous studies have reported that TPase becomes active on D-Ser in the presence of triammonium phosphate (TAP) to make the enantioselectivity flexible. TAP is the most important among ammonium phosphates because it gives TPase the highest activity on D-Ser. The presence of TAP promotes a small conformational change to TPase to fit D-Ser partly into the catalytic site of the active site and help D-Ser to form the external aldimine bond with PLP. This subtle steric interaction, whose detail is still being investigated, are very necessary to transform D-Ser from inhibitor into active substrate. Future research will determine a metabolic pathway of L-Trp synthesis from D-Ser, and also demonstrate the formation of an aldimine bond between amino group of D-Ser and PLP at the first step of this reaction in the presence of TAP.

CO6-2 Study of Localization Estimation of Abasic Sites in DNA Irradiated with Ionizing Radiation

K. Akamatsu, N. Shikazono and T. Saito¹

Irradiated Cell Analysis Research Group, Quantum Beam Science Research Center, Japan Atomic Energy Agency (JAEA)

¹Research Reactor Institute, Kyoto University

INTRODUCTION:

DNA lesions induced by ionizing radiation and chemicals can cause mutation and carcinogenesis. In particular, “clustered damage” site, that is a DNA region with multiple lesions within one or two helical turns, is believed to hardly be repaired. This damage is considered to be induced, e.g., around high-LET ionizing radiation tracks. However, detail of the damage is not known. We have already developed a method for estimating degree of localization of abasic sites (APs) in DNA using Förster resonance energy transfer (FRET). The FRET efficiency (E) was calculated using the donor fluorescence intensities before/after enzymatic digestion of the labeled AP-DNA [1]. First, we have applied the method to $^4\text{He}^{2+}$ (2.0 MeV/u, LET: ~ 70 keV/ μm)- $^{12}\text{C}^{5+}$ (0.37 MeV/u, LET: ~ 760 keV/ μm)- and ^{60}Co γ -irradiated DNA in the solid state. The results showed that $^{12}\text{C}^{5+}$ beam likely produced close APs within a track. The apparent distance calculated from the E value was approximately 17 base pairs [2]. This finding indicates that *direct radiation effect* of $^{12}\text{C}^{5+}$ beam near the Bragg peak produces clustered DNA damage. We have recently applied the method to DNA in a cell-mimetic radical scavenging condition [3,4]. Here, we show new results using $^4\text{He}^{2+}$ beam and ^{60}Co γ -rays.

EXPERIMENTS:

•Sample preparation and He beam irradiation

The plasmid DNA digested by Sma I was used (linear form). The DNA was dissolved to be 0.1 g/L in 0.2 M Tris-HCl buffer (pH 7.5) which is a cell-mimetic condition in relation to radical scavenging capacity. One hundred microliters of the DNA solution was transferred to an irradiation folder [2], and was irradiated with the $^4\text{He}^{2+}$ beam (12.5 MeV/u, LET: ~ 19 keV/ μm ; TIARA, JAEA), and ^{60}Co γ -rays (LET: ~ 0.2 keV/ μm ; Kyoto University Research Reactor Institute: KURRI) were also used as a standard radiation source.

•Preparation of fluorophore-labeled irradiated DNA and the FRET observation

The irradiated DNA (10 μL in water) and 10 μL of 100 mM Tris-HCl (pH7.5) were mixed in a microtube. Two microliters of a mixture containing AF350 (donor fluorescent probe) and AF488 (acceptor one) with a given molar ratio was added to the DNA solution and was incubated for 24 h at 35°C. The fluorophore-labeled DNA was purified by precipitation by ethanol. Twenty

microliters of water was added to the residue. The fluorescence intensities were measured both at 449 nm (ex. 347 nm for AF350) and at 520 nm (ex. 460 nm for AF488). After the measurement, the enzyme cocktail containing DNase I and phosphodiesterase I was added to the solution, followed by being incubated for 3 h at 37°C. E values were calculated from the donor intensity before/after the digestion.

RESULTS AND DISCUSSION:

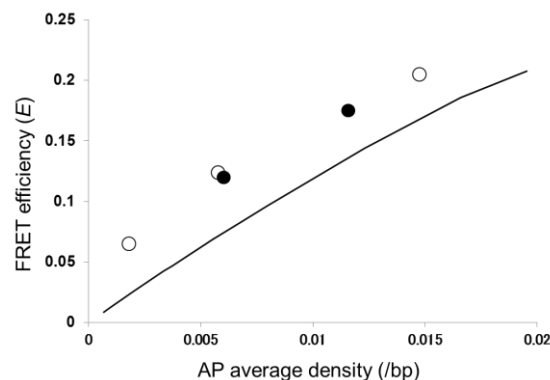


Fig. 1. Relationship between AP average density and FRET efficiency for He ion beam (●) and ^{60}Co γ -rays (○). The solid line indicates a theoretical curve for randomly-distributed APs in DNA.

As shown in Fig.1, there was no difference in FRET efficiency (E) between the two radiation sources. But interestingly, all data points were above the curve for random distribution. This finding suggests that AP distribution for the γ -rays as well as that for the He beam is not completely random. This tendency is similar to the result using dry DNA as sample for irradiation [2]. A radiation “spur” on or nearby DNA might sometimes produces clustered damage. In any case, knowledge of AP distribution for ^{60}Co γ -rays as a reference is quite important to study DNA damage by ionizing radiation. More data points and discussions will be needed to elucidate the problem.

REFERENCES:

- [1] K. Akamatsu, N. Shikazono, Anal. Biochem. **433** (2013) 171-180.
- [2] K. Akamatsu, N. Shikazono, and T. Saito, Radiat. Res. **183** (2015) 105-113.
- [3] K. Akamatsu, N. Shikazono, and T. Saito, KURRI Progress Report 2012 (2012) 256.
- [4] K. Akamatsu, N. Shikazono, and T. Saito, KURRI Progress Report 2012 (2013) 263.

Suzuki T.¹, Horie K.¹, Ogawa S.¹, Wakamatsu E.¹,
Abe R.¹, Sakurai Y.², and Ono K.²

¹Research Institute of Biomedical Sciences,
Tokyo University of Science

²Research Reactor Institute, Kyoto University

INTRODUCTION: Boron neutron capture therapy (BNCT) is an attractive therapy for local tumor control in the treatment of brain tumor, melanoma, and so on [1,2]. However, some important issues are remained: the tumor-specific accumulation of highly concentrated boron, the real-time quantification of boron concentration in local tumor tissues, and the prevention of re-growth and metastasis of residual tumor cells after BNCT.

Recently, it was reported that some cancer immune therapies could achieved significant regression of tumor in clinical trials. To achieve successful tumor regression, in this study, we try to establish the combination treatments with BNCT and immunotherapy [3,4].

Results and Discussions:

The effect of BNCT on immune system

Using mouse model, we examined the effect of BNCT on the antigen specific immunological response. C57BL/6 mice, which were subcutaneously administrated with 250 mg/kg BPA, and then treated with thermal neutron irradiation (1 MW, 50min in the heavy water facility of KUR). To assess the immune response, mice were immunized with antigen on footpad, and the immunological response of T cells was assessed (Fig.1A). Although transient lymphopenia was observed after neutron irradiation, the number of immune cells was restored at 11 days after treatment. Assessing IFN- γ production, the antigen specific immune response was comparable in neutron irradiated mice, compared with control mice (Fig. 1B), suggesting that antigen-specific immune response could be induced even after neutron irradiation.

Anti-tumor immune response after BNCT

It was previously reported that local X ray radiotherapy lead to the augmentation of anti-tumor immune response via the induction of inflammation and immunological cell death in tumor site [5]. Hence, we examine anti-tumor immune response in hosts which received BNCT or X ray radiotherapy. Mice were challenged B16 melanoma cells on leg, and, BNCT or local X ray irradiation (12Gy) therapy were performed around 10 days after tumor challenge. Fourteen days after radiation therapy, immune response against tumor derived antigen was assessed (Fig.2 A). As a result, similar to previous reports, anti-tumor immune response was augmented by radiotherapy with X ray (data not shown).

Notably, unlike X ray irradiation, BNCT did not enhance anti-tumor immune response. Although additional immunization with peptide vaccination and CTLA4 blockade after BNCT lead to the induction of immune response, this combination therapy could not achieve tumor regression (Fig.2B and 2C). Our further interest is why BNCT could not enhance anti-tumor immune response. To understand the anti-tumor immune response during radiation therapy determines the effective combination with radiation therapy and immune therapy.

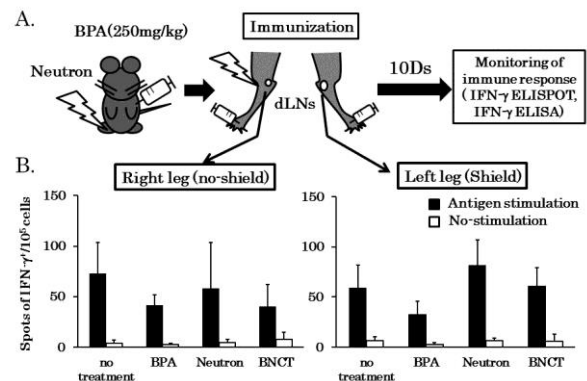


Fig 1. Antigen-specific immune response could be induced after neutron-beam irradiation. A: schema of experiment. B: Immunological responses (IFN- γ production of T cells) in draining lymph node (dLNs).

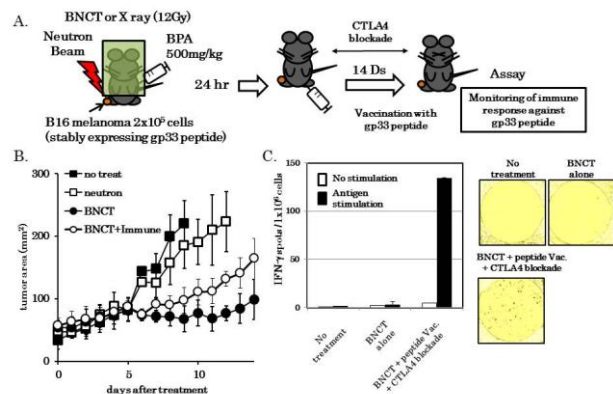


Fig. 2. Anti-tumor immune response after BNCT or radiotherapy with X ray, but not BNCT, augmented immune response against tumor derived antigens. A: Schema of treatment for tumor bearing mice. B: Tumor growth. C: Number of IFN- γ producing cells against tumor derived antigens

REFERENCES:

- [1] M. Suzuki, *et al.* Int. J. Radiat. Oncol. Biol. Phys. 58(3): 892-896, 2004.
- [2] M. Suzuki, *et al.* Int. J. Radiat. Oncol. Biol. Phys. 60(3): 920-927, 2004.
- [3] Lifu Dengu *et al.*, J. C. I., 124 (2), 687, 2014.
- [4] M. A. Curran *et al.*, PNAS, 107(9), 4275, 2010.
- [5] Lionel A. *et al.*, Nature Med., 13(9), 1050, 2007

採択課題番号 26049 BNCT の免疫に与える影響と免疫療法による全身治療との併用の可能性 通常採択
東理大・生命研) 安部 良、鈴木利宙、小川修平、若松 英、堀江和峰 (京大・原子炉) 櫻井良憲、
小野公二

CO6-4 *In situ* Visualization of Boron in Plants Using Neutron Capture Radiography

M. Kobayashi and T. Kinouchi¹

Graduate School of Agriculture, Kyoto University

¹Research Reactor Institute, Kyoto University

INTRODUCTION:

Boron (B) is an essential micronutrient for vascular plants, and its deficiency is one of the major constraints on crop production worldwide [1]. Boron deficiency causes various physiological disorders including an inhibition of the development of young leaves, necrosis of tissues inside tubers or tap roots, or failure in seed set.

The understanding of physiological function of B in plants has progressed greatly during the last few decades. Boron as boric acid occurs in cell wall, and forms 1:2 borate-diol diester with specific regions of pectin [2]. The diester bonds serve as the inter-chain bridges of pectin, thereby stabilizes the cell wall structure. On the other hand, the transport and distribution of B in plant remains elusive, since no radioactive isotope with an appropriate half-life is available for this element. Revealing a differential distribution of B within tissues, if any, may give us clues to the demands for B of different cell types, hence may contribute significantly to a better understanding of the physiological role of B. Thus, in this study we have been trying to apply boron neutron capture radiography to the *in situ* visualization of B in plant roots.

EXPERIMENTS:

Radish (*Raphanus sativus* L. *sativus*) seeds were germinated on vermiculite in a growth chamber with a light/dark regime of 18/6 h, 22°C, and 60% relative humidity. Seedlings with uniform size were transferred to solution culture, which was maintained in the same growth chamber. The nutrient solution contained B at 0.5ppm. At 10 days after transfer to solution culture, the tap roots were detached from the seedlings and fixed with glutaraldehyde. Fixed samples were embedded in OCT compound (Tissue-Tek), frozen in liquid nitrogen, and sectioned at 8- μ m thickness with freezing microtome. The ultrathin sections were transferred onto CR-39 nuclear track detector. The bright-field image of the section was taken at this point, to record the structure of tissue examined. The CR-39 plate was then irradiated with neutron for 15 min using Te-Pn facility at Kyoto University Research Reactor Institute. The irradiated CR-39 plate was etched in NaOH solution, and the resulting pits were observed under microscope.

RESULTS AND DISCUSSION:

When the image of pits generated by neutron irradiation was merged with the section image taken prior to the irradiation, the pits were distributed unevenly over the section. Higher density of pits was found in the central

part and a circular region just inside the cortex, which are the regions rich in vascular bundles. Boron as borate diester is specifically bound to the rhamnogalacturonan II (RG-II) regions of pectin in cell wall, and the RG-II has been shown to occur in all cells of the roots at the same density [3]. Thus the distribution of B within roots seems distinct from that of its acceptor molecule.

Besides borate diesters bound to RG-II regions of pectin, B in plants can occur as free boric acid as well, when the plants are amply fed with B [4]. The free boric acid in shoots corresponds to B taken up as luxury absorption beyond the amount equivalent to that of the acceptor. Radish seedlings used in this study were grown in the presence of enough amount of B, and hence they were likely to contain both RG-II-bound and free boric acid. At present, we are not sure to which fraction of B the signals in radiography are ascribed. However, the observed pattern of pit distribution seems inconsistent with those expected for bound B: since the acceptor RG-II occurs ubiquitously and evenly within the root, the bound B is also expected to occur uniformly. Taken together, we think that the signal detected in this study probably came from soluble, free boric acid in root tissues.

Radish deficient in B sometimes accumulates a blue pigment in the roots, which is called "Ao-aza" (blue spot) symptom. Interestingly, the regions where the blue pigment (presumably anthocyanin) accumulates overlap with those showing signals in this study. It is suggested that cells in the regions may require higher supply of B than the others. In the vascular bundles occurs cambium, which contains the cells actively propagating. Higher supply of B may be necessary to support rapid cell proliferation in these tissues.

As the subject of future investigation, it is necessary to make clear which fraction of B (cell wall-bound or free boric acid) has been detected in this radiography. Growing plants under various B supply to prepare samples with different content of free boric acid, then examining the pit frequency would give useful information on this aspect. In addition, increasing the sensitivity and resolution is also necessary. Optimizing the condition of neutron irradiation or alkaline etching would be useful to solve these problems.

REFERENCES:

- [1] V.M. Shorrocks, *Plant Soil*, **193** (1997) 121–148.
- [2] M. Kobayashi *et al.*, *Plant Physiol.*, **110** (1996) 1017–1020.
- [3] T. Matoh *et al.*, *Plant Cell Physiol.*, **39** (1998) 483–491.
- [4] T. Matoh *et al.*, *Soil Sci. Plant Nutr.*, **47** (2001) 779–784.

CO6-5 Measurement of Transmittance Spectra of a Cryo-Sectioned Tissue of Brain Tumor C6 Model in the Sub-Terahertz Region-II

N. Miyoshi and T. Takahashi¹

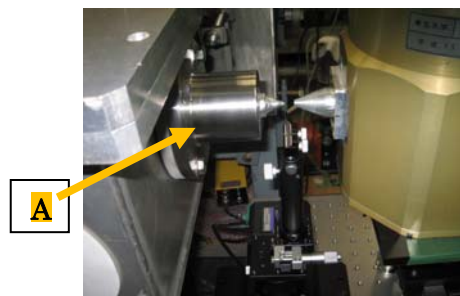
Department of Tumor Pathology, Faculty of Medicine,
University of Fukui

¹ Research Reactor Institute, Kyoto University

INTRODUCTION: The LINAC (linear particle accelerator) technology in the millimeter and terahertz waves had been unique and had been used as a coherent synchrotron light in the research reactor institute of Kyoto university (KURRI) to observe the transmittance spectra of a sectioned tissue of raw brain tumor C6 model as a collaborate study. The absorption spectra in the sub-terahertz region had been not so clear for the raw tumor tissue although Ashworth-PC. *et al.* [1] had reported for the excised human breast cancer by a terahertz pulsed spectroscopy observed at 320 GHz, which was estimated a longer relaxation time component of the induced electricity for water molecules [2-3] in the raw tumor tissue for three years at the linear analysis.

We also estimated what kind of water molecules become dominant in the viable and necrotic cancer regions by the different measurement method as an aim of 2D mapping study.

EXPERIMENTS: (1) Instrument of Near-field in tera-hertz region: The photograph of the instrument was shown in **Figure 1**. Mark-A: Pre-probe Wiston cone; 50-10mm diameter, Length=60mm; the irradiate diameter=0.775mm; The concentrate light probe (diameter)=3mm. The instrument was developed by Dr. T. Takahashi in KURRI [Figure-1] for the 2D mapping analysis.



(2) Sample preparation: A cryo-sectioned (thickness=100 μm) tissue was prepared from the raw C6 glial tumor model using a Cryo-section Maker (Leica) and was sealed sandwich-type with saran-wrap film (thickness=10 μm), under freezing condition (-20 C) before the measurements.

RESULTS: Large amount of spectroscopic data (more than 1,000) for the 2D mapping data have been analyzed to now, but the analysis was not finished to be reported as the imaging of each water components.

REFERENCES:

- [1] Phillip C. Ashworth, *et al.*, *Optics Express*, **17(14)**: 12444-12454 (2009).
- [2] Toshiko Fukasawa, *et al.*, *Phys. Rev. Let.*, **95**: 197802 (2005).
- [3] Hiroyuki Yada, *et al.*, *Chem. Phys. Let.*, **464**: 166-170 (2008).

CO6-6 Design and Synthesis of New Drugs for Boron Neutron Capture Therapy and Boron Magnetic Resonance Imaging

S. Aoki¹, Y. Nishiura¹, T. Tanaka¹, Y. Hisamatsu¹, Y. Sawamoto¹, Rikita Araki², Takaomi Saido³, T. Suzuki⁴, K. Horie⁴, Ryo Abe⁴, S. Masunaga⁵, K. Natsuko⁵, Y. Sakurai⁵, and K. Ono⁵

¹Faculty of Pharmaceutical Sciences, Tokyo University of Science

²Bruker Biospin K. K.

³RIKEN Brain Science Institute

⁴Research Institute of Biomedical Sciences, Tokyo University of Science

⁵Research Reactor Institute, Kyoto University

INTRODUCTION: Boron neutron capture therapy (BNCT) is one of powerful therapies for local tumor control in the treatment of brain tumor, melanoma, and so on [1]. However, some important issues are remained for the achievement of successful tumor regression: the tumor-specific accumulation of highly concentrated boron, the real-time quantification of boron concentration in local tumor tissues, and the prevention of re-growth and metastasis of residual tumor cells after BNCT. In this study, we have designed and synthesized new boron compounds appended with macrocyclic tetramines such as cyclen (1,4,7,10-tetraaminocyclododecane) for BNCT and B-MRI [2]. It was expected that boron clusters such as icosahedral carboranes would be transferred to living cells due to the dicationic properties of cyclen part at neutral pH.

Icosahedral carboranes are boron clusters composed with 10 boron atoms and 2 carbon atoms which exhibit a remarkable thermal and chemical stability. In this manuscript, we reported first example of full deboronation reaction of *o*-carborane catalyzed by copper(II) ion. Initially, we examined the deboronation reaction of *ortho*-carborane-cyclen in aqueous solution in the presence of various d-block metals such as Cu²⁺, Zn²⁺, Fe²⁺, Ni²⁺ and Co²⁺.

EXPERIMENTS and RESULTS:

Synthesis of boron compound based on

Boron is one of ultratrace elements in living systems. Previously, we have designed and synthesized boron-pendant cyclic tetraamine **1** for the in-cell ¹¹B NMR (nuclear magnetic resonance) or MRI (magnetic resonance imaging) for the detection of metal in living systems and eventually for the use in BNCT. It was reported that the C-B bond is hydrolyzed upon complexation with d-block metals to give one molecule of boric acid (B(OH)₃) as well as zinc complex of *N*-benzylcyclen **2**

[3].

These results prompted us to design and synthesize its analog (**3**) having an icosahedral carborane (*o*-carborane) unit that consist 10 borons and 2 carbons as a potent carrier of boron cluster to the cancer cells. It was found that this molecule is transferred into cancer cells more effectively than **1**. Moreover, we have discovered that the *o*-carborane unit of **3** decomposes in the presence of d-block metals in aqueous solution at neutral pH and release more than 4 molecules of B(OH)₃ [4]. Besides, *o*-carborane analog **4** having methanol unit instead of cyclen also undergoes the full decomposition to release 10 B(OH)₃. This change was successfully detected on ¹¹B NMR and MRI. Because the chemical and physical properties of ¹⁰B and ¹¹B are almost identical, these probes should be useful not only for BNCT, but also for the determination of the distribution of boron-containing drugs in the bodies and of the biorelevant d-block metals.

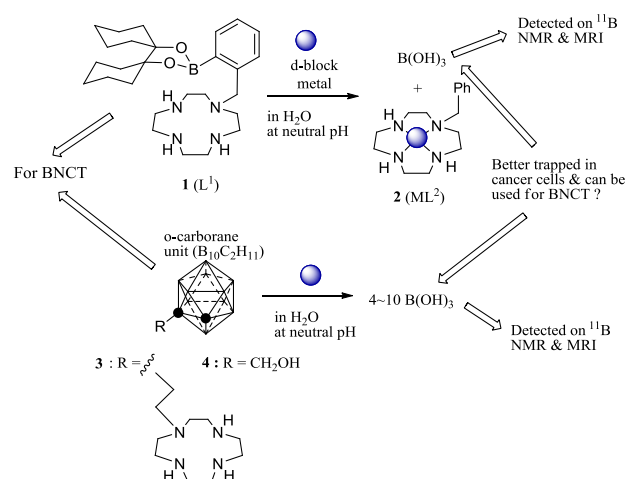


Fig 1. Design and decomposition reaction of boronylated compounds

REFERENCES:

- [1] a) R. F. Barth *et al.*, *Clin. Cancer Res.*, **11** (2005) 3987-4002. b) R. F. Barth *et al.* *Rad. Oncol.* **7** (2012) 146-166.
- [2] a) G. W. Kalbalka, *et al.* *J. Neuro-Oncol.* **33** (1997) 153-161. b) P. Bendel, *NMR in Biomed.* **18** (2005) 74-82.
- [3] M. Kitamura *et al.*, *Inorg. Chem.* **50** (2011) 11568-11580.
- [4] Y. Nishiura *et al.*, Manuscript in preparation.

採択課題番号 26077

がん組織に集積する含ホウ素化合物の設計・合成と腫瘍への集積のホウ素 MRI に向けた基礎検討

通常採択

(東理大・薬学部) 青木 伸、西浦由紀子、田中智博、久松洋介、澤本泰宏

(ブルカーバイオスピン) 荒木力太 (理研) 西道 隆臣 (東理大・生命研) 鈴木利宙、堀江和峰、安部良 (京大・原子炉) 増永慎一郎、近藤夏子、櫻井良憲、小野公二